International Communications in Heat and Mass Transfer 68 (2015) 27–31

Contents lists available at ScienceDirect

International Communications in Heat and Mass Transfer

journal homepage: www.elsevier.com/locate/ichmt

Evaluation of thermal performance of graphene overcoat on multi-layered structure subject to laser heating☆

Peng Yu *, Shengkai Yu, Weidong Zhou

*Data Storage Institute, Agency for Science, Technology and Research (A*STAR), DSI Building, 5 Engineering Drive 1, Singapore 117608*

ARTICLE INFO

Available online 28 August 2015

Keywords:
Multi-layered structure
Laser heating
HAMR
Graphene

ABSTRACT

The present study investigates heat transfer on the multi-layered structure with graphene overcoat induced by laser heating. The thermal performance of graphene overcoat is compared with that of diamond like carbon (DLC) overcoat. The temperature rise is lower in the structure with graphene overcoat, which is due to the lower laser energy absorption rate and the higher in-plane thermal conductivity of graphene. The presences of interfacial thermal resistance and surface convection may have more significant effects on the structure with graphene overcoat.

1. Introduction

Heat-assisted magnetic recording (HAMR) is a promising technique to circumvent the obstacle from superparamagnetic effect, and to achieve higher storage density on the order of 10 Tb/in^2 [1]. The HAMR media is of very high coercivity, which is not writable by using conventional write head at the room temperature. To reduce the coercivity, a laser beam is imposed on a tiny region of the recording media and rapidly heats it above the Curie temperature (about 700 K) during writing cycle. The temperature field on the disk thus becomes highly non-uniform around the region heated by the laser beam. The unknown effect of laser heating on the structural stability of the overcoat layer on disk media is of great concern.

The challenge of further increase in the areal recording density of a hard disk drive (HDD) includes the reduction in the gap between the head and the recording layer. To achieve the areal density on the order of 10 Tb/in^2, the thicknesses of the lubricant layer and the overcoat layer are requested to reduce to ~1 nm and ~2 nm, respectively. Diamond like carbon (DLC) is considered as a promising overcoat for HDD under HAMR conditions due to its outstanding properties. It is known that DLC can be deposited at room temperature. The properties of DLC range between those of diamond and graphite, which (e.g. density ρ, heat capacity C_p and thermal conductivity κ) can be tuned by changing the sp^3 content, the organization of the sp^2 sites, and the hydrogen or nitrogen content [2–4]. However, the reliability of DLC films for HAMR application is still under discussion due to the effect of laser irradiation on thermal stability of DLC overcoat [5]. The demand for novel and ultrathin overcoat for HAMR condition is still persistent.

Graphene, a two-dimensional crystal formed by a single layer of carbon atoms, may be a good candidate for the overcoat for HAMR applications. The thickness of a single layer graphene is about 0.3354 nm. Compared with DLC overcoat of 2-4 nm, using graphene as an overcoat layer can significantly reduce the gap between the head and media. The intralayer strong sp^2 bond gives graphene remarkable mechanical properties [6,7]. The Young's modulus of a suspended single layer of graphene is remarkably high of ~ 1 TPa, which is one of the stiffest known materials. Other properties of graphene, such as superior electronic conductivity and thermo-mechanical response [7–9], may also potentially improve areal density in HDDs [10].

In HAMR application, the laser is introduced to heat a very small region of the multi-layered structure. The multi-layered structure usually consists of a recording layer and other function layers, which is typically protected by a thin overcoat layer. Understanding the underlying physics of the local unsteady heat transfer induced by laser heating in such applications is of critical importance. Using DLC overcoat as an example, Yu et al. [11] have shown that the thermal and optical properties of the overcoat material are important design factors for HAMR applications. It is known that the thermal and optical properties of grapheme are different from those of DLC. Therefore, it is also important to evaluate the thermal effect of graphene overcoat on the multi-layered structure, which is the main objective of the present study.

The organisation of the rest of the paper is as follows. Section 2 describes the governing equations, boundary conditions, numerical techniques as well as the thermal and optical properties of graphene and other materials. Section 3 presents the numerical results on the thermal performance of graphene overcoat, as well as a comparison with the thermal performance of DLC overcoat. Finally, a conclusion is drawn in Section 4.

☆ Communicated by W.J. Minkowycz.

* Corresponding author at: Institute of High Performance Computing, Agency for Science, Technology and Research (A*STAR).
E-mail address: yup@ihpc.a-star.edu.sg (P. Yu).

http://dx.doi.org/10.1016/j.icheatmasstransfer.2015.08.005
0735-1933/

2. Numerical method

In the present study, we concern the thermal performance of a graphene overcoat layer, which is deposited on the top of the multi-layered structure, on local temperature increase induced by laser heating. The application background for the present study is data storage industry. Fig. 1 shows a schematic of the corresponding multi-layered structure, which consists of substrate, graphene overcoat and several other function layers. DLC overcoat is also considered in the present study for the purpose of comparison.

The thermal and optical properties of the materials involve in the present study are summarized in Table 1, in which ρ, C_p, κ, N, and δ are density, heat capacity, thermal conductivity, complex refractive index ($N = Nr - i{\cdot}Ne$, Nr and Ne are the real and imaginary parts of the complex refractive index, respectively), and thickness, respectively. In the present study, we assume that the thermal and optical properties are temperature independent. The complex refractive index is a function of the laser wave length. We consider the laser wave lengths of 632 nm and 850 nm in the present study. The material properties, except those for graphene, are either found in literature [11,12] or measured by the equipments in Data Storage Institute.

The properties of graphene are difficult to be obtained due to the feature of two-dimensional crystal. The thickness of a single layer of graphene is about 0.335 nm. The density and the specific heat are adopted as those for graphite (maybe regarded as 3D version of graphene), which are 2.25 g/cm^3 and 700 J/(kg K), respectively. The in-plane and out-plane thermal conductivities of graphene are quite different, which are 2000 W/(m K) and 6 W/(m K) [13], respectively. The refractive index of a single layer of graphene can be approximated by the equation [14]

$$n = \sqrt{1 - i\frac{a\lambda}{28}}, \tag{1}$$

where λ is the wave length and α is the fine structure constant, which is equal to 1/137 [15].

A laser beam with wave length λ and power P_W is shot onto the structure. The laser beam may move against the media, which reflects the relative motion of the rotating disk and the laser. The laser heating in the multi-layered media is often considered as the heat flux boundary condition at the media surface [16,17]. However, the propagation of the laser wave in the multi-layered structure is described by the Maxwell equation in the present study [18]. The electric and magnetic fields in each layer can be obtained by solving the Maxwell equation. The rate of flow of laser energy $S_k(z)$, where the subscript k denotes the number of layer from the bottom to the top and the variable z (Cartesian coordinate) denotes the depth measured from the top of the multi-layered structure, through the multi-layered structure can be calculated by

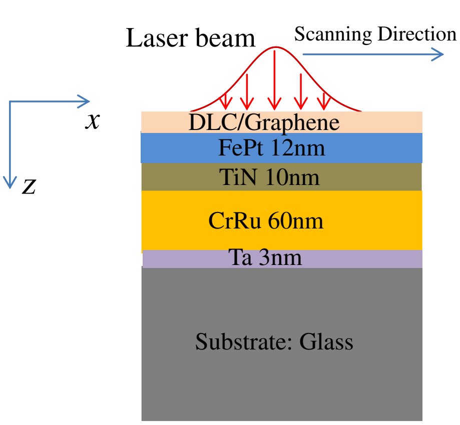

Fig. 1. Typical structure of multi-layered media (not to scale).

invoking the Poynting vector theorem [18]. Note that $S_k(z)$ can be determined by the thickness and the optical property (the complex refractive index) of each layer. If the laser intensity distribution in the x-y plane can be expressed by the Gaussian function, the local heat generation rate can then be yielded, which is incorporated into the energy equation by a source term [19,20],

$$\frac{\partial T}{\partial t} = \alpha_k \nabla^2 T - \frac{1}{\rho_k C_{Pk}} \frac{P_W}{\pi r^2} \frac{dS_k(z)}{dz} e^{-\frac{(x-x_0)^2 + (y-y_0)^2}{r^2}} \tag{2}$$

where t is time, T is the temperature, α_k, ρ_k, C_{pk} are the thermal diffusivity, the density, and the specific heat capacity of the kth layer medium, x, y, z are Cartesian coordinates, x_0 and y_0 are the spatial coordinates for the centre of the laser beam, which moves related to the rotating disk, and r is e^{-1} radius of the Gaussian beam. In the present study, we only consider the motion of laser spot in the x-direction and the laser spot is initially located at the origin (0, 0) of the top surface. The variation of x_0 with time can be expressed as $x_0 = u_L{\cdot}t$, where u_L is the scanning speed of laser. The zero speed of the laser ($u_L = 0$) means stationary heating.

The e^{-1} radius of laser beam is $r = 250$ nm, and the power is $P_W =$ 15 mW. The laser beam moves at a speed $u_L = 10$ m·s^{-1} related to the rotating disk. The laser is turned on at $t = 0$ and kept on. The temperature on the disk initially shoots up and then gradually approaches a constant with the elapse of time. Both adiabatic and convective heat transfer conditions are considered at the top surface. The computational domain is set to be 50r × 50r in the x and y directions while 500 nm in the z direction. This computational domain is proved to be large enough and have a negligible effect on the overall accuracy of the numerical solution. Thus, the constant ambient temperature is composed at all boundaries excerpt the top surface. A finite volume method based on the Cartesian grid is used to solve the governing equations. A second order implicit scheme in time and a second-order central difference scheme in space are applied to discretize the governing equations. The grid size and time step applied in the present study are also fine enough to capture the major transport phenomena. The validation of the numerical method has been presented in our previous work [12,19] and will not be repeated here.

3. Results and discussion

The electromagnetic energy of the laser wave is absorbed by the multi-layered structure when the wave propagates through the structure. The absorption rate does not depend on the intensity of the laser. Fig. 2 presents the laser energy flow rate along the z direction in the multi-layered structure. Only the energy flow rate up to the depth of $z = 100$ nm is shown because it approaches zero when $z > 100$ nm. Generally, 30% - 40% of laser energy is transferred into the multi-layered structure and absorbed locally, which is dependent on the wave length of the laser. For the same structure, the laser absorption rate is higher for the wavelength of 632 nm. For the same wavelength, the structure with DLC absorbs more laser energy. Table 2 records the details on the energy absorption rate at each layer. For the wavelength of 632 nm, the DLC layer absorbs more laser energy and also promotes the energy absorption in other layers, compared with the graphene layer. For the wavelength of 850 nm, the DLC layer only promotes the energy in other layers while the absorptions in the DLC and graphene layers are identical.

The temperature distribution on the structure varies with time and position because the laser beam moves above the multi-layered structure. However, if the reference frame is fixed at the centre of laser beam, the temperature distribution would reach a nearly quasi-steady state after the initial shooting-up period. In the present study, we only present the temperature profiles or fields at the quasi-steady state (at $t = 40$ ns). The temperature showed actually is the temperature increase against the ambient temperature (308 K). This temperature